ISSN : 0974 - 7524 Volume 7 Issue 4

Trade Science Inc.

Physical CHEMISTRY
An Indian Journal

Full Paper

PCAIJ, 7(4), 2012 [143-147]

ZnO compounds thickness-related optimality on bases of blue-red-shifts and Urbach tailing

A.Amlouk, K.Boubaker*, M.Amlouk

Unité de physique des dispositifs à semi-conducteurs, Faculté des sciences de Tunis, Université de Tunis El Manar, 2092 Tunis, (TUNISIE)

PACS: 61.05.cp, 61.72.-y, 66.30.J-, 78.30.Fs 81.05.Dz, 82.80.Pv

ABSTRACT

In this study, the spray pyrolysis system has been selected to grow ZnO crystals of different thicknesses. The existence of a critical thickness has been already conjectured on the bases of optothermal and mechanical investigations. Energy levels shifts within ZnO forbidden band along with Urbach tailing perturbed evolution have been analyzed in order to explain and justify the already conjectured thickness-related optimality.

KEYWORDS

ZnO;
TCO;
Red shift;
Blue shift;
Spray technique;
Micro-hardness;
Optimization;
Urbach tailing;
Intrinsic defects;
Shallow levels;
Deep levels;
Energy level diagram.

INTRODUCTION

ZnO is a II-VI crystal semiconductor with band wide gap energy of 3.37 eV[1-8]. Its direct band structure is suitable for optoelectronic devices such as light emitting diode (LED) and laser diode (LD) used in ultra violet and blue region. Due to its low cost as well as its favorable opto-electronic and electro-luminescent properties, this oxide has been successfully incorporated in fluid sensing devices[9], acoustic devices[10], transparent electrodes[11], and solar cells[12-16]. During the last decades, ZnO compound have been prepared through several methods[17-26] including pulsed laser deposition (PLD), chemical vapour deposition (CVD), RF magnetron sputtering, direct current (DC) magnetron reactive sputtering,co-electro-deposition and sol-gel technique.

In this work, the spray pyrolysis system, with the advantages of low cost, simple processing and practically controllable growth rate, has been selected to prepare ZnO crystals using, as main precursor, a solution of zinc acetate dissolved in de-ionized water. The thickness-dependent performance of the different as-grown crystals layers has been investigated in terms of morphological, opto-thermal and micro-hardness behaviours. Additional investigations of the induced red shift and Urbach tailing evolution confirmed trends toward existence of a thickness-related optimality.

EXPERIMENTAL DETAILS PURE

Zinc oxide crystals have been prepared by the tech-

nique of chemical reactive technique in liquid phase spray. The obtained layers' structural and morphological properties, as well as synthesising details, have been detailed in recent publications[27-30].

ZnO crystals layers were fabricated at different thicknesses (samples $S_i|_{i=1..6}$ with thicknesses d=0.16, 0.4, 0.58, 0.64, 0.84 and 1.03 μm respectively) on glass substrates. Precursor solution and gas flow rates were kept constant at 2 $cm^3.min^{-1}$ and 4.0 $l.min^{-1}$ respectively. The substrate temperature was fixed at the optimal value (T_s=460°C). The optimality of this temperature has been verified in previous studies[28-29].

RESULTS AND DISCUSSION

A synopsis of XRD, mechanical and opto-thermal characterization

XRD, mechanical and opto-thermal characterization of the as-grown crystals have been previously achieved[23-25]. XRD patterns of the deposited ZnO layers (Figure 1) showed i. e. that the thinner layers $S_i|_{i=1..4}$ monitored a preferred orientation of the crystallites with respect to the (002) reflection. Differently, the thicker ones: S_5 and S_6 presented two additional XRD peaks: (101) and (100) besides the existent (002) with a loss of crystallinity in concordance with results recorded by Tneh *et al.*[31], Herklotz *et al.*[32], Ryu *et al.*[33].

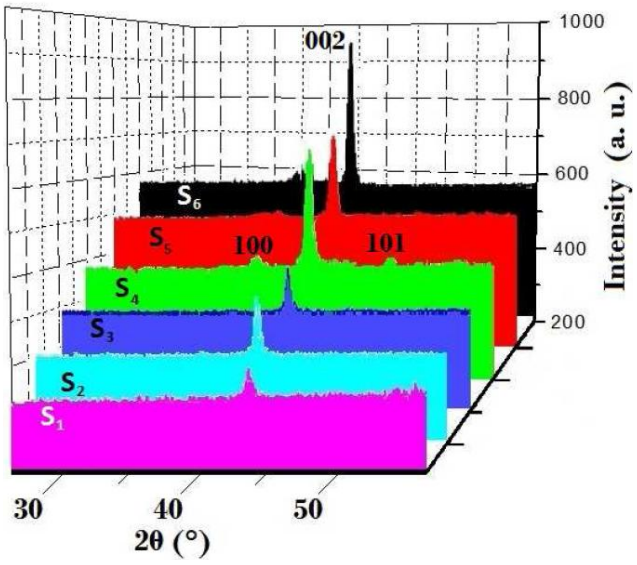

Figure 1 : XRD patterns of the deposited ZnO crystals layers

Thickness dependent red shift and Urbach tailing

Urbach energy E_u has been determined through the equations:

$$\begin{cases} \mathrm{Ln}(\alpha(h\nu)) = \mathrm{Ln}(\alpha_0) + \dfrac{h\nu}{E_u} \\ E_u = \alpha(h\nu)\left(\dfrac{d[\alpha(h\nu)]}{d[h\nu]}\right)^{-1} = h\left[\dfrac{d}{d\nu}(\mathrm{Ln}\,\alpha(\nu))\right]^{-1} \end{cases} \quad (1)$$

Where $\alpha(h\nu)$ represents the experimentally deduced optical absorption profile.

The width of the localized states (band tail energy or Urbach energy E_u) has been estimated from the slopes of $(Ln\alpha(\nu))$ vs energy $h\nu$ plots of the films $S_i|_{i=1..6}$ (Figure 2).

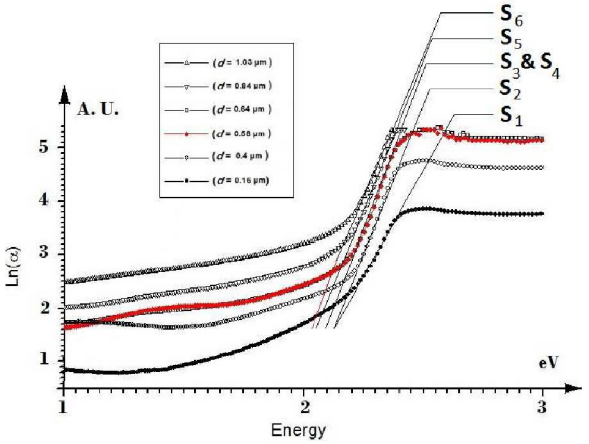

Figure 2 : Of $Ln\alpha$ versus energy $h\nu$ plots as guides to determine Urbach energy

Energy band analyses

Like elemental semiconductors, binary ZnO properties have their genesis in both intrinsic and extrinsic effects. Intrinsic transitions occur between electrons in the conduction band (CB) and holes in the valence band (VB), while extrinsic properties depend on point defects and impurities. In ZnO crystalline structure, the main native defects like Zinc vacancy (V_{Zn})ACC, interstitial Zinc (Zn_i) and Oxygen vacancies (V_O), often create supplementary electronic states in the bandgap (Figure 3) resulting in Urbach tailing at both conduction and valence edges vicinity.

Among the native defects, interstitial Zinc (Zn_i) and Oxygen vacancies (V_O) have been particularly pointed by Van de Valle[34] as low-energy native point defects that cause difficulties of making p-type ZnO. Several

photoluminescence studies[35-37] showed that undoped ZnO yielded red photoluminescence is originated in a transition from a shallow state (SL) to a deep level(DL). Cao *et al.*[36] and Lin *et al.*[37] identified these states as Zn_i for SL and V_O for DL while Look.[38], Jin *et al.*[39], Pöppl *et al.*[40] attributed to both entities the role of SL shallow donor.

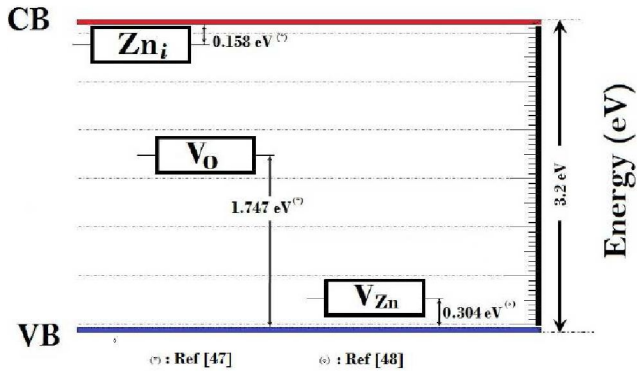

Figure 3 : ZnO energy level diagram

According to recent investigations of Zhang *et al.*[41] and F. Kohan *et al.*[42] who verified that interstitial zinc has no deep levels inside ZnO gap[11–13], and therefore acts as shallow effective-mass double donor,, it seems that unanimity on Zn_i status is reached.

From another point of view, it has been proven[34,43,44] that deviation from ordinary stoichiometry (Zn excess) causes interstitial Zn^{2+} (radius≈0.78Å) to occupy either ordered positions causing tail decrease, or random positions inside the crystal, resulting in the recorded over-limit Urbach tailing. In this context, we tried to calculate Urbach energy of the samples from data of Figure 2. The thickness-dependent values of E_u are presented in Figure 4.

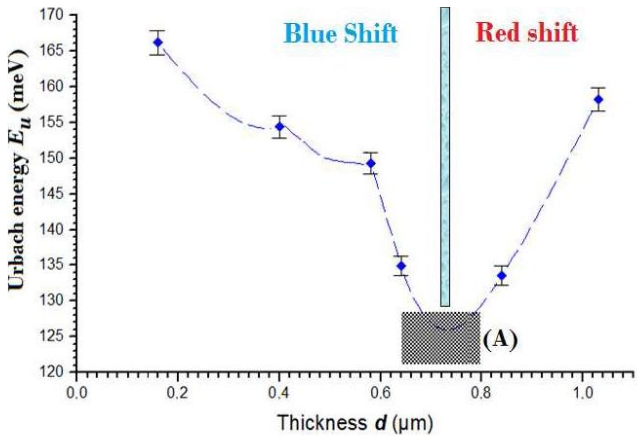

Figure 4 : Of $Ln\alpha$ versuss energy *hv* plots as guides to determine Urbach energy

A simple comparison between Figures 3 and 4 shows that the decrease of E_u recorded for the thinner layers $\mathbf{S_i}|_{i=1..4}$ is equivalent to the lack of Zn_i resulting in maintained values of the bandgap along with a pronounced blue shift. This phenomenon is in perfect concordance with XRD patterns of these samples which show an unperturbed (002) direction trend. For thicker layers S_5 and S_6, the red-shift caused by increasing E_u toward values close to Zn_i-CB gap (≈0.150 eV) means that beyond a given thickness interstitial Zinc is more and more predominant.

A second look to these samples XRD patterns allows confirming that peaks other than (002) appear. Since no new material has been supplied, these peaks can be attributed to diffusion of Zn_i inside the würtzite matrix causing the recorded loss of crystallinity (§3.1).

A conjectured[45], critical thickness ($d_{cr.}$ ≈0.656 µm) has been proposed in a study concerning the same samples. The values obtained from Eq. 1 and the energy level diagram confirm the range of this thikness (Figure 3, detail (A)).

Concerning the second donor candidate V_O, studies published by Vlasenko[46], Mass[47] and Gavryushin[48] confirm the uncertainty about the shallowness of its energy level. It has been shown that dispersed values of 0.94, 1.6, 1.82 and 2.48 meV beyond VB have been recorded. In our study, E_u values did not exceed 200 meV, however some measurements effectuated on a 2.1 µm ZnO sample yielded high values of E_u (≈ .82 eV) along with amorphousness features. These last results confirm precedent analyses[49-50] the recorded increasing contribution of V_O to the bandgap tailing in relatively thick ZnO layers (i. e. O_2 sensing layers).

CONCLUSION

In this study, we have investigated the thickness-dependent evolution of un-doped ZnO layered crystals deposited by a low cost technique. The already discussed notion of critical thickness has been discussed in terms of behaviours of intrinsic native shallow and deep donors energy levels within the valence-conduction bandgap. Blue-shift and red-shift records along with Urbach tailing evolution presented a verifiable explanation to the mor-

phological changes observed beyond a given thickness. Comparison with already proposed positioning and interpretation of some native pont defects outlined the role of interstitial zinc Zn_i as a shallow donor in the post-criticality phase. More investigations are needed in order to evaluate Zinc vacancy (V_{Zn}) and Oxygen vacancies (V_O) contribution to Urbach tailing amplitude.

REFERENCES

[1] F.K.Shan, G.X.Liu, W.J.Lee, B.C.Shin; J.of Crystal Growth, **291**, 328 **(2006)**.

[2] S.R.Aghdaee, V.Soleimanian; J.of Crystal Growth, **312**, 3050 **(2010)**.

[3] J.Young Park, J.Ho Je, S.Sub Kim; J.of Crystal Growth, **312**, 3588 **(2010)**.

[4] T.M.Trad, K.B.Donley, D.C.Look, K.G.Eyink, D.H.Tomich, C.R.Taylor; J.of Crystal Growth, **312**, 3675 **(2010)**.

[5] G.Nan He, B.Huang, H.Shen; J.of Crystal Growth, **312**, 3619 **(2010)**.

[6] N.Bouhssira, M.S.Aida, A.Mosbah, J.Cellier; J.of Crystal Growth, **312**, 3282 **(2010)**.

[7] W.E.Mahmoud; J.of Crystal Growth, **312**, 3075 **(2010)**.

[8] A.AbuEl-Fadl, E.M.El-Maghraby, G.A.Mohamad; Cryst.Res.Technol., **39**, 143 **(2004)**.

[9] M.Suchea, S.Chiritoulakis, K.Moschovis, N.Katsarakis, G.Kiriakidis; Thin Solid Films, **515**, 551-566 **(2006)**.

[10] W.Water, S.Y.Chu, Y.D.Juang, S.J.Wu; Mater.Lett., **57**, 998-1004 **(2002)**.

[11] F.Michlotti, A.Belardini, A.Rousseau, A.Ratsimihety, G.Schoer, J.Mueller; J.Non-Cryst.Solids, **352**, 2339-2344 **(2006)**.

[12] J.Hupkes, B.Rech, O.Kluth, T.Repmann, B.Zwayagardt, J.Muller, R.Drese, M.Wutting; Sol. Energy Mater.Sol Cells, **90**, 3054-3066 **(2006)**.

[13] S.Nagae, M.Toda, M.Minemoto, H.Takakura, Y.Hamakawa; Sol.Energy Mater.Sol Cells, **90**, 3568-3575 **(2006)**.

[14] N.Phuangpornpitak, S.Kumar; Renew. & Sust. Energy Rev., **1**, 1530-1543 **(2007)**.

[15] S.Rehman, I.M.El-Amin, F.Ahmad, S.M.Shaahid, A.M.Al-Shehri, J.M.Akhashwain, A.Shash; Renew.& Sust.Energy Rev., **11**, 635-653 **(2007)**.

[16] W.J.Jeong, S.K.Kim, G.C.Park; Thin Solid Films **506–507**, 180-199 **(2006)**.

[17] J.Bandara, C.M.Divarathne, S.D.Nanayakkara; Sol.En.Mat.Sol.Cells, **81**, 429-437 **(2004)**.

[18] A.Alkaya, R.Kaplan, H.Canbolat, S.S.Hegedus; Renew.Energy, **34**, 1595-1599 **(2009)**.

[19] J.Montero, J.Herrero, C.Guillén; Sol.En.Mat.Sol. Cells, **94**, 612-616 **(2010)**.

[20] T.Sands, V.G.Keramidas, R.Gronsky; Washburn J.Mater.Lett, **3**, 409-13 **(1985)**.

[21] H.J.Liu, Y.C.Zhu; Mater.Lett., **62**, 255-7 **(2008)**.

[22] Y.Y.Xi, T.L.Y.Cheung, H.L.Dickon; Ng.Mater. Lett., **62**, 128-32 **(2008)**.

[23] Wang, R.Liu, A.Pan, S.Xie, B.Zou; Mater.Lett., **61**, 4459-62 **(2007)**.

[24] Y.Khoptiar, I.Gotman; Mater.Lett., **57**, 72-6 **(2002)**.

[25] G.X.Liu, F.K.Shan, W.J.Lee, B.C.Shin, H.S.Kim, J.H.Kim; Ceramics Intern., **34**, 1011-15 **(2008)**.

[26] H.Hallil, P.Ménini, H.Aubert; Procedia Chemistry, **1**, 935-938 **(2009)**.

[27] B.Ouni, J.Ouerfelli, A.Amlouk, Boubaker, K.M.Amlouk; J.of Non-Cryst.Solids, **356**, 1294-99 **(2010)**.

[28] A.Amlouk, K.Boubaker, M.Amlouk, M.Bouhafs; J.Alloys Comp., **485**, 887-891 **(2009)**.

[29] A.Amlouk, K.Boubaker, M.Amlouk; J.Alloys Comp., **490**, 602-604 **(2010)**.

[30] S.Dabbous, T.Ben Nasrallah, J.Ouerfelli, K.Boubaker, M.Amlouk, S.Belgacem; J.Alloys Comp., **487**, 286-292 **(2009)**.

[31] S.S.Tneh, Z.Hassan, K.G.Saw, F.K.Yam, H.Abu Hassan; Physica B., **405**, 2045-2048 **(2010)**.

[32] F.Herklotz, E.V.Lavrov, J.Weber; Physica B, **404**, 4807-4809 **(2009)**.

[33] B.Ryu, K.J.Chang; Physica B, **404**, 4823-4826 **(2009)**.

[34] C.G.Van de Walle; Phys.Rev.Lett., **85**, 1012 **(2000)**.

[35] Ü.Ozgür, Y.I.Alivov, C.Liu, A.Teke, M.A. Reshchikov, S.Dogan, V.Avrutin, S.J.Cho, H.Morkoc; J.Appl.Phys., **98**, 041301 **(2005)**.

[36] B.Cao, W.Cai, H.Zeng; Appl.Phys.Lett., **74** 161101 **(1999)**.

[37] B.Lin, Z.Fu, Y.Jia; Appl.Phys.Lett., **79**, 943 **(2001)**.

[38] D.C.Look; Mater.Sci.Eng.B, **80**, 383 **(2001)**.

[39] B.J.Jin, S.H.Bae, S.Y.Lee, S.Im; Mater.Sci.Eng.B, **71**, 301 **(2000)**.

[40] A.Pöppl, G.Völkel; Phys.Status Solidi A, **125**, 571 **(1991)**.

[41] S.B.Zhang, S.H.Wei, A.Zunger; Phys.Rev.B, **63**, 075205 **(2001)**.

[42] A.F.Kohan, C.Ceder, D.Morgan, C.G.Van de Walle; Phys.Rev.B, **61**, 15019 **(2000)**.

[43] S.W.Xue, X.T.Zu, W.L.Zhou, H.X.Deng, X.Xiang, L.Zhang, H.Deng; J.Alloys Comp., **448**, 21-26 **(2008)**.
[44] Y.Pan, F.Inam, M.Zhang, D.A.Drabold; Phys.Rev. Lett., **100**, 206403-11 **(2008)**.
[45] A.Amlouk, K.Boubaker, M.Bouhafs, M.Amlouk; J.of Crystal Growth, Submitted, **(2010)**.
[46] L.S.Vlasenko; Physica B, **404**, 4774–4778 **(2009)**.
[47] J.Mass, M.Avella, J.Jiménez, A.Rodríguez, T.Rodríguez, M.Callahan, D.Bliss, Buguo Wang; J.of Crystal Growth, **310**, 1000 **(2008)**.
[48] V.Gavryushin, G.Račiukaitis, D.Juodžbalis, A.Kazlauskas, V.Kubertavičius; J.of Crystal Growth, **138**, 924 **(1994)**.
[49] K.Boubaker; Mat.Sci.Engin.A MSEA, **528**, 1455-1457 **(2011)**.
[50] A.Amlouk, K.Boubaker, M.Bouhafs, M.Amlouk; Journal of Alloys and Compounds,